

Response to Reviewer 1:

We would like to thank the reviewer for the constructive feedback on our manuscript and for aiding our progress towards publication. These comments were very useful, and we appreciate the time taken to help improve the paper. Each comment is repeated here, and our responses are given below each one in blue text. Excerpts from the text of the paper are given in *italics*, where **new additions are bolded** and text removed is noted using ~~strikethrough~~. All line numbers mentioned in our responses correspond to the line numbers in the updated version of the manuscript. Figures provided to answer reviewer questions are labelled as A, B, C, etc. to not be confused with numbered figures in the manuscript.

Lenhardt et al. investigate the effects of above-cloud and below-cloud CCN concentrations on cloud-top properties, primarily using remote sensing measurements obtained during the ORACLES campaign. The datasets used in this study, along with the co-location methodology (Figure 2), are clearly described and well justified. The calculation of ACI metrics is also comprehensively presented. The manuscript is well written and easy to follow. Uncertainty quantification is clearly described for both the physical properties and the regression slopes. I have a few minor comments that aim to further improve the manuscript. I recommend it for publication after these comments are addressed.

Thank you for the constructive and positive feedback on our study!

Minor comments:

1. Lines 63-65: The limitations also include 3D scattering, which enhances near cloud reflectance and is maximum for sunlit edges of clouds (Varnai and Marshak 2009, 2011). Active lidar observations are not affected by such 3D effects.

T. Vrnai and A. Marshak, "MODIS observations of enhanced clear sky reflectance near clouds", *Geophys. Res. Lett.*, vol. 36, pp. L06807, Mar. 2009.

T. Varnai and A. Marshak, "Global CALIPSO Observations of Aerosol Changes Near Clouds," in *IEEE Geoscience and Remote Sensing Letters*, vol. 8, no. 1, pp. 19-23, Jan. 2011, doi: 10.1109/LGRS.2010.2049982.

Thank you for pointing this out. The following sentence was added in Lines 69-71: ***“Enhanced near-cloud reflectance due to three-dimensional scattering can also occur at sunlit cloud edges (Varnai and Marshak, 2009; 2011), which does not impact active lidar observations.”*** Additionally, these papers were added to the references list.

2. Lines 99-103: Do all airborne measurements used in this study correspond to clouds influenced by smoke plumes? If so, please explicitly state this in the research questions. Also in line 102, change “Nccn concentration” to “Nccn”

Yes, all observations correspond to clouds impacted by smoke. To make this clearer in the research questions, question 1 was revised to the following in Lines 112-113: ***“1. Can remote sensing retrievals replicate the relationships between above-cloud N_{CCN} and cloud***

top microphysical properties identified from in situ measurements for clouds impacted by smoke aerosols?”

The “concentration” typo in question 3 was also removed.

3. Equation 1: it would be more convenient for readers to use 10^{-6} than $e-06$

Equation 1 was edited to contain a 10^{-6} instead of $e-06$.

4. Figure 1: Do the authors consider only those flight snippets that contain clouds when estimating the autocorrelation? If not, I recommend restricting the analysis to such segments, since the conclusion that CCN concentrations do not vary significantly over horizontal distances of 5 km is used to support the representativeness of cloud-adjacent regions in depicting below-cloud concentrations.

Thank you for pointing out this important detail/consideration. Our initial analysis did not distinguish between clear-sky vs. below-cloud flight segments. Here we show a comparison between these cases, where we have used changes in SSFR downwelling solar radiation to categorize flight segments that at any point made observations below-cloud (Fig. A). We find that, as expected, below-cloud processing/precipitation scavenging of aerosols results in a lower CCN autocorrelation coefficient than in clear-sky regions. However, considering the below-cloud autocorrelation coefficient remains, on average, above 0.9 out to 5 km, we feel this is high enough to maintain our assumption of constant below-cloud N_{CCN} over lengths of 5 km from cloud edge. Also to note in Fig. A is the decrease in autocorrelation around 1.5 km that is followed by an increase for the below-cloud analysis. We hypothesize that this is due to a statistical limitation of data availability and varying lengths of the flight segments used in the analysis. We plan to continue this assessment in future work and take more time to carefully consider what is causing this discrepancy. As a result of this analysis, we added the following to the manuscript:

- Line 253-260: *“First, the constant altitude flight legs below 500 m and 1000 m likely include both clear-sky and below-cloud observations. **In a separate analysis, we distinguished clear-sky observations from below-cloud observations using changes in downward solar radiation and found that effects of cloud processing result in decreased N_{CCN} autocorrelation in below-cloud observations when compared to clear-sky observations. However, the autocorrelation coefficient remained, on average, above 0.9 at lags between 0 and 5 km (not shown), suggesting reasonable correlation for both below-cloud and clear-sky observations. While not a focus of this study, we plan to expand on these differences between clear-sky and below-cloud N_{CCN} autocorrelation in a future analysis.** , and such cases are not differentiated before being included in this analysis. Additionally, those that flight segments were observed below-cloud...”*

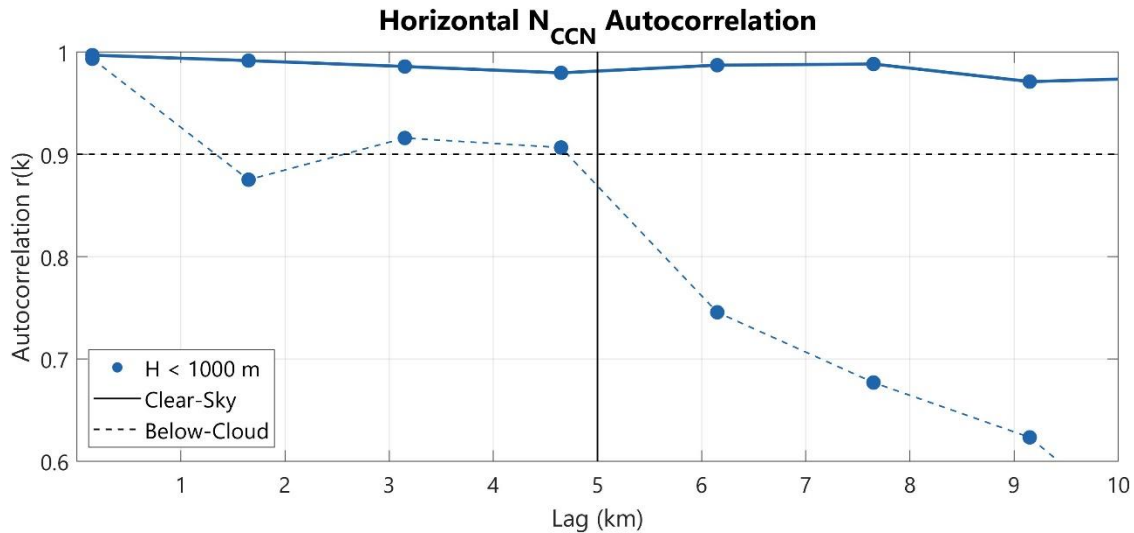


Figure A. Horizontal CCN autocorrelation for observations made at $H < 1000$ m for clear-sky (solid line) and below-cloud (dashed line) flight segments.

Additionally, while our original autocorrelation analysis in the manuscript included lines for $H < 500$ m and $H < 1000$ m, we have consolidated to only one line for $H < 1000$ m to capture the layer where most cloud bases fall. Flights made at $H < 500$ m are also captured in $H < 1000$, but considering this layer as a separate analysis is difficult to interpret since there are significantly fewer data pairs observed at $H < 500$ m. Therefore, we felt that having two separate lines did not add enough useful information to the analysis. This change has been made in the manuscript figure (Fig. 1) as well. Corresponding to this adjustment, the following edits were made in the text:

- Figure 1 caption: “The autocorrelation coefficient of in situ N_{CCN} observed in horizontal flight legs is given as a function of lag distance. The ~~light blue line~~ represents observations from flight legs at altitudes (H) below 500 m, the dark blue line represents observations from flight legs at altitudes (**H**) below $H < 1000$ m, and the red line represents observations from flight legs between $H = 1000$ -2000 m. The black dashed line depicts an autocorrelation coefficient of 0.95, and the solid vertical line depicts the 5 km over which we assume that below-cloud N_{CCN} is approximately constant.”
- Line 233-234: “...we calculate autocorrelation for constant altitude flight legs flown at altitudes below 1000 m ~~and at altitudes below 500 m~~ to capture the range...”
- Line 240: “Additionally, we find that N_{CCN} autocorrelation remains ~~above~~ close to 0.95...”

5. Line 300: MERRA 2 data citation needs correction:

Global Modeling and Assimilation Office (GMAO) (2015), MERRA-2 inst3_3d_asm_Np: 3d,3-Hourly,Instantaneous,Pressure-Level,Assimilation,Assimilated Meteorological Fields V5.12.4, Greenbelt, MD, USA, Goddard Earth Sciences Data and Information Services Center (GES DISC), Accessed: [Data Access Date], 10.5067/QBZ6MG944HW0

The details for this citation were changed in the reference list and in Line 324-325.

6. Equations 7 and 8: I suggest also stating the physical meaning of these ACI metrics. For instance, $d\ln N_d/d\ln N_{CCN}$ represents the fractional change in cloud droplet number concentration in response to a fractional change in CCN concentration. It may also be noted that these quantities are fundamental components of radiative forcing calculations. Thank you for this suggestion. The following sentence was added in Lines 349-352: ***“Here, Eq. (7) describes the fractional change in cloud top R_{eff} in response to fractional changes in N_{CCN} at a constant LWP and Eq. (8) captures the fractional change in cloud droplet N_d when there is a fractional change in N_{CCN} . Such ACI metrics describe cloud microphysical responses to aerosol perturbations and are critical components in cloud radiative forcing calculations (McComiskey et al., 2009; Ghan et al., 2016).”*** The Ghan et al. (2016) reference was also added to the reference list.

Additionally, the following edits were made for clarity in the following sentence (Lines 352-354): ***“These values ACI_{REF} and ACI_{CDNC} correspond to the slope of linear regressions calculated for log-transformed R_{eff} , N_d , and N_{CCN} , and here these regressions are calculated for all data points (not the bin averages).”***

7. Is it possible that above-cloud and below-cloud CCN concentrations are correlated? If so, could the observed correlation between above-cloud CCN concentrations and cloud properties be biased by this co-variability?

We have investigated the relationship between above- and below-cloud N_{CCN} for the cloud edge cases where we look at the simultaneous impact of both. This comparison is shown below as a density plot with a best fit line from a linear regression also included (Fig. B). Since there is no clear linear relationship, we do not expect that any such co-variability is significantly biasing the observed above-cloud N_{CCN} – cloud property correlation. We have also added the following sentence to lines 465-467 of the revised manuscript:

“Additionally, an investigation of the relationship between above- and below-cloud N_{CCN} did not show significant correlation between the two, and we do not hypothesize that the observed correlation between above-cloud N_{CCN} and cloud properties is highly biased by a co-variability with below-cloud N_{CCN} .”

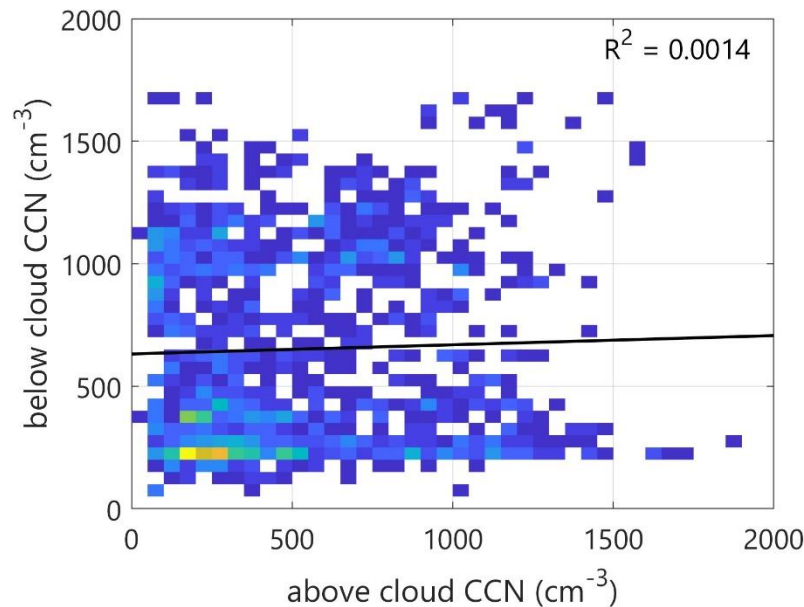


Figure B. Density plot of above- vs. below-cloud N_{CCN} within the CE dataset.

8. I am surprised by the low ACICDNC value of 0.053 estimated from below-cloud CCN and cloud-top N_d . This implies that for every 100% increase in below-cloud CCN, N_d increases by only 5%. If I understand the methodology correctly, below-cloud CCN is approximated using CCN concentrations adjacent to clouds, which is what satellite-based studies assume in ACI studies. However, this sensitivity is considerably lower than values reported from satellite observations, including those based on active lidar, which typically range between 0.3 and 0.4 (e.g., Zheng et al., 2025; Li et al., 2025; Choudhury et al., 2026). The authors should comment on this discrepancy. In addition, the strong meteorological dependence of ACI metrics reported by Zheng et al. (2025) is not evident in Figure B1 in the Appendix for below-cloud CCN and cloud-top N_d .

One possible explanation is that the presence of an aerosol plume above the cloud, which may actively serve as a CCN reservoir for the cloud-top or boundary, as also shown by Gupta et al. (2021), makes the cloud-top N_d less related to below-cloud CCN. This could be also discussed in Line 475.

Zheng, X., Feng, Y., Painemal, D., Zhang, M., Xie, S., Li, Z., Jacob, R., and Lusch, B.: Regimebased aerosol–cloud interactions from CALIPSO-MODIS and the Energy Exascale Earth System Model version 2 (E3SMv2) over the Eastern North Atlantic, *Atmos. Chem. Phys.*, 25, 17473–17499, <https://doi.org/10.5194/acp-25-17473-2025>, 2025.

Li, Z., Painemal, D., Feng, Y., and Zheng, X.: Progress in the quantification of aerosol-cloud interactions estimated from the CALIPSO-CloudSat-Aqua/MODIS record, EGU sphere [preprint], <https://doi.org/10.5194/egusphere-2025-4769>, 2025.

Choudhury, G., Goren, T., & Tesche, M. (2026). Satellite observations show negligible impact of mineral dust on cloud droplet number. *Geophysical Research Letters*, 53, e2025GL120234. <https://doi.org/10.1029/2025GL120234>

We would like to thank the reviewer for the comments and thoughts about this weak below-cloud N_{CCN} relationship with cloud microphysical properties and acknowledge that the manuscript should have more directly addressed and interpreted the implausibility of such a weak relationship. Based on figure visualization suggestions from both reviewers, we found more of a noticeable trend/pattern in what was originally Figure B1 and have moved this figure to the main text as Figure 9. A further discussion of our interpretation of this updated figure and associated changes to the manuscript are located at the end of this document (“Below-Cloud Edits” section).

In short, we found that at high LTS the below-cloud N_{CCN} has a stronger relationship with cloud properties than seen using the above-cloud N_{CCN} . The CE dataset primarily represents low LTS environments, so without constraining by LTS, low-LTS/weak-ACI observations dominate the below-cloud results as shown in Figure 7 of the manuscript. Additionally, the CE analysis can be influenced by stronger cloud edge/cloud top entrainment mixing, which may lead to weaker correlations between below-cloud N_{CCN} and cloud top microphysical properties, as seen in previous studies. The SEA is a unique regime in which both above- and below-cloud N_{CCN} can simultaneously modulate cloud properties, and separating their respective effects from observations is non-trivial. One of our main goals in this study is to demonstrate that large-scale remote sensing observations show similar effects to those found from an in situ study. While we believe that LTS differences, enhanced entrainment at cloud edges, and the uniqueness of this regime all play a role in explaining the low ACI metrics calculated for the full CE dataset, there are a few other key differences between our study and these three satellite papers that may cause discrepancies.

First, all three approaches estimate aerosol relative to cloud using only cloud top, or defined/fixed layers, while our method estimates a cloud base with which to determine below-cloud N_{CCN} on a profile by profile basis. This likely gives a more realistic estimate of above- and below-cloud aerosol loading than is available from a satellite-based approach. Second, Zheng et al. (2025) averages over 25 km tracks and Li et al. (2025) averages over 25 x 25 km boxes. Since we are using a much smaller spatial resolution (lidar observations with a 2 km horizontal resolution), this could also cause differences, especially as our below-cloud analyses are limited to within 5 km of cloud edge, where COT and LWP are low, while these other approaches are likely to average over a wider (higher) range of cloud properties. Below is an estimate of the above- vs. below-cloud N_{CCN} comparison using an approach where we averaged cloud properties within a 25 km radius of any clear-sky,

cloud-adjacent lidar profile (Fig. C). Though still lower than the above-cloud ACI metrics, averaging over a larger spatial scale does increase the below-cloud N_{CCN} ACI metrics from 0.032 to 0.062 for ACI_{REF} and 0.053 to 0.151 for ACI_{CDNC} . Therefore, another possible reason for discrepancy between this study and satellite lidar approaches may be the difference in averaging scales. Lastly, Zheng et al. (2025) and Li et al. (2025) do not correct from ambient to dry extinction, so in humid regions this extinction approach is likely to overestimate aerosol loading, which may bias the ACI metrics.

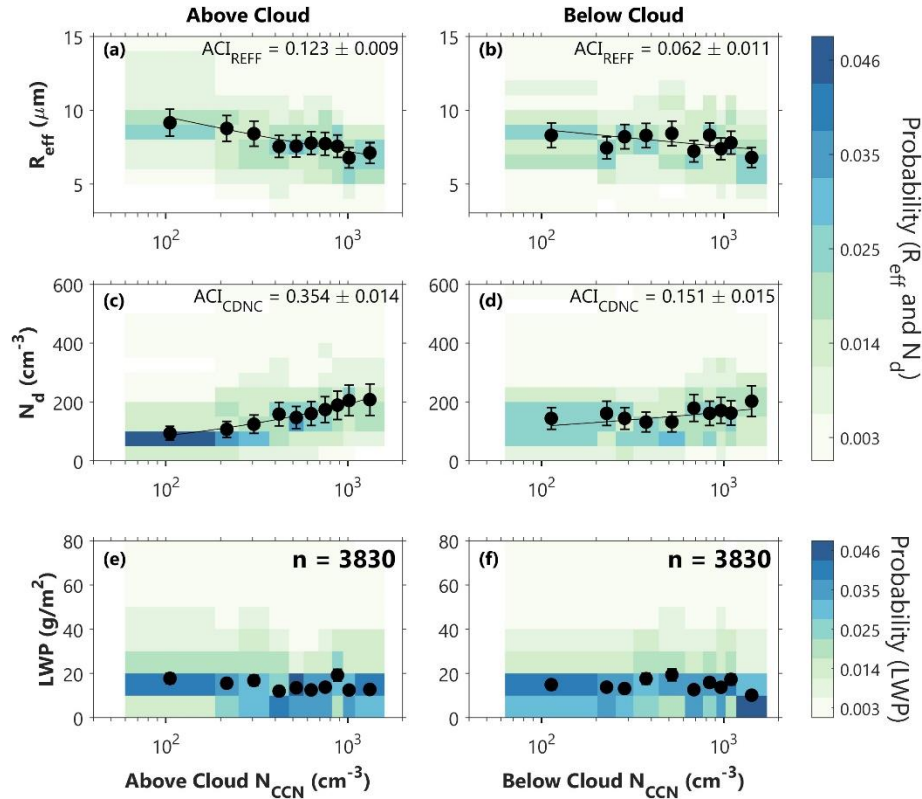


Figure C. Figure 4 from the manuscript plotted for an approach that averages cloud top microphysical properties within a 25 km radius circle of any clear-sky, cloud-adjacent lidar profile.

9. As a general comment, I recommend using an alternative binning approach in Figures 4, 5, 7, 8, and 10. Instead of fixed N_{ccn} bins, consider dividing the dataset into a specified number of equally populated bins based on N_{ccn} , and then estimating the median Y value within each bin. This approach can improve the visual representation of the relationship between X and Y. Additionally, using a logarithmic scale for the X-axis may further improve these figures.

We would like to thank the reviewer for this suggestion! We agree that this binning approach does improve the visual representation of these relationships. Each of those figures now have 10 bins of equal population and medians are shown instead of mean values. What was previously figure B1, that is now Figure 9, uses the same approach.

However, in Figure 9 we use fewer bins in the last two clusters to reduce noise due to having fewer observations compared to the first two columns.

As a result of changing figures to use this binning approach, some figure interpretations needed to be adjusted in the writing. These changes are primarily related to the pattern reversal we saw in Fig. 4 at $CCN > 1000 \text{ cm}^{-3}$ and are outlined here:

- There was a small typo in how the ACI metrics in Fig. 4 were originally calculated. Therefore, we made the following changes in line 372: “ ACI_{REF} is **0.101** ~~0.093~~ and ACI_{CDNC} is **0.282** ~~0.275~~...”
- In the first version of Fig. 4, there was more of a steady increase in LWP at $CCN > 1000 \text{ cm}^{-3}$, but with the new binning method these appear more as small fluctuations without as obvious a trend. Therefore, the wording in lines 374-375 was slightly changed: “While LWP is limited to 0-80 g/m^2 , we still see some fluctuations in the LWP **as with changes in N_{CCN} increases** (Fig. 4c)...”
- The Fig. 4 caption was adjusted to now read as: “Relationship between above-cloud N_{CCN} and (a) R_{eff} , (b), N_d , and (c) LWP across all three ORACLES deployments. Shading in the background represents the probability of where the 9223 individual data points from this AC data set fall within each panel. **Data are separated into 10 bins such that each bin contains an equal number of data points.** Each scatter point **represents the median cloud property is an average within an above-cloud each individual N_{CCN} bin of 300 cm^{-3} .** The size of the scatter point represents the ~~number of data points that fall within the bin, and~~ The error bars represent the **average median** uncertainty of the respective cloud property within that bin. ACI metrics and their SE (\pm) are given for R_{eff} and N_d . The fit lines correspond to the slope determined by each ACI metric.”
- Lines 365-362 (original line numbers) were removed in the updated manuscript. These discussed the reversal in cloud property responses, which are no longer evident when each bin contains an equal number of data points.

Other minor figure interpretations/descriptions in Section 3 that were edited because of the changed binning approach are outlined here:

- Line 341-345: “For Fig. 4 and those like it in the remainder of Sect. 3, shading on the figures show probability distributions of where individual data points fall, while the ~~larger~~ scatter points represent ~~an average~~ the median of each cloud property within ~~ten~~ N_{CCN} bins **determined such that each bin contains an equal number of data points of 300 cm^{-3} .** The size of the scatter point is a visual representation of the ~~relative number of data points within each N_{CCN} bin, and~~ The error bars give the **average median** uncertainty of each cloud property within that bin.”
- Line 416-417: “while clusters 2 and 3 show mostly constant LWP with an increase for $N_{CCN} > 1000 \text{ cm}^{-3}$ **the highest N_{CCN} bin in cluster 2.**”
- Line 447-449: “The range of average N_{CCN} in the 500 m below-cloud is of similar magnitude as N_{CCN} in 100 m above cloud, **with fewer clean cases below-cloud**”

than above-cloud, which is likely evidence of entrainment mixing of BBA from the smoke plume into the BL.”

- The Figure 8 caption was corrected to show $n = 1249$ instead of 1174, a previous typo that hadn't been caught.

Since the pattern reversal (the increase in R_{eff} and decrease in N_d for $\text{CCN} > 1000\text{cm}^{-3}$) is no longer evident in Fig. 4 but is still visible in the highest CCN bin of cluster 2 in Fig. 5, we have left the possible hypotheses for what may cause this in Section 4 (now Sect. 4.2, titled “Reversals in expected patterns”). However, some of the text around these was edited and reframed as follows:

- Lines 573-580: *“There are **a few** small scale variations evident in the bin averages medians that are not significantly reflected in the fit lines and therefore are not a primary focus of this analysis. **These patterns could be an artifact of retrieval uncertainties. However, here we will discuss a few alternative hypotheses based on previous literature. However For example, in Fig. 4a and 4b, as well as Fig. 5b and 5f, we see a slight-reversals in the expected patterns for increase in R_{eff} and decrease in N_d for the highest concentration N_{CCN} bin above-cloud $N_{\text{CCN}} > 1000\text{ cm}^{-3}$. These bin averages have fewer data points and slightly higher mean uncertainty than those at lower N_{CCN} , meaning that this switch to increasing R_{eff} and decreasing N_d for high above-cloud N_{CCN} could be an artifact of uncertainty and limited data. However, here we will discuss a few alternative hypotheses based on previous literature. For example, c- Considering this pattern only occurs at $N_{\text{CCN}} > 1000\text{ cm}^{-3}$...”***
- Line 594: *“...also associated with increasing R_{eff} and decreasing N_d here (Fig. 4c and Fig. 5j).”*

Below-Cloud Edits

Upon replotting Figure B1 according to the binning and colorbar changes suggested by Reviewers 1 and 2, an LTS-dependence of the below-cloud N_{CCN} relationship with cloud properties was more evident compared to how it was plotted originally. In this figure, we now see more clearly the opposite pattern as observed in Figure 5, where cloud sensitivity to increasing below-cloud N_{CCN} increases as LTS increases. Additionally, once these cloud edge observations are split into LTS regimes, there are very few that fall in the cluster with the highest LTS. Therefore, we argue that the weak below-cloud response evident in Figure 7 is because the dataset is dominated by samples within the relatively low LTS regimes, and the high LTS response being washed out when combined with the entire CE dataset.

Therefore, we have moved Figure B1 to Section 3.2 as the new Figure 9 and added the following paragraph:

“Lastly, we investigate the LTS dependence of the below-cloud N_{CCN} relationship to cloud top microphysical properties using a similar approach as in Fig. 5. Data from the CE data set are assigned to the existing clusters determined from AC data set so that both analyses are directly comparable. These results are shown in Fig. 9, where we observe from the fit lines and ACI metrics a trend inverse of that observed for the above-cloud N_{CCN} . That is, as LTS increases, the sensitivity of cloud properties to increasing below-cloud N_{CCN} increases. This suggests that in less stable environments, entrainment mixing of above-cloud BBA into the cloud layer is the dominant process responsible for the microphysical changes to stratocumulus cloud properties. However, in more stable environments, where vertical mixing is suppressed and low-level cloud cover increases, the lack of such entrainment mixing results in a stronger response of cloud properties to increasing below-cloud N_{CCN} . Another important finding from this analysis is that most observations in the CE dataset fall into the first two clusters characterized by relatively low LTS. Therefore, when considering the total impact of below-cloud N_{CCN} across all clusters, as done in Fig. 7, low LTS cases dominate the analysis, explaining why the relationship between cloud properties and below-cloud N_{CCN} appears as weak and nearly negligible.”

Section 4.1 was also edited to include a more in-depth discussion of the differing LTS dependencies and physical relationships for above- and below-cloud N_{CCN} . This section was re-titled as “Above- vs. below-cloud N_{CCN} relationships.” These changes and additions are outlined below:

“4.1 ~~Physical relationships~~ Above- vs. below-cloud N_{CCN} relationships

*Overall, the relationships analyzed here follow the major findings of Gupta et al. (2021), around which this study was formulated. That is, for cases where the smoke plume is in contact with the cloud top, there is evidence of these CCN impacting cloud top microphysical properties. For all cases, increases in above-cloud N_{CCN} were associated with increases in N_d and decreases in R_{eff} . Cases of contact between cloud top and the BBA plume are associated with greater entrainment mixing (Diamond et al., 2018; Gupta et al., 2021), and our finding here reiterates those suggesting that entrainment of BBA that serve as CCN can result in nucleation of cloud droplets near the cloud top. **These relationships are evident regardless of BL aerosol loading, with a slightly dampened impact of above-cloud N_{CCN} in cases where the BL is relatively polluted.** Additionally, we found*

~~relatively weak relationships between below-cloud N_{CCN} and cloud top microphysical properties, but an indication that polluted BL conditions were associated with a dampened above-cloud N_{CCN} impact. However, it is important to consider that the above- and below-cloud N_{CCN} comparisons in this study were limited to observations within 5 km of cloud edge, and thus they may not be perfectly representative of below-cloud N_{CCN} impacts closer to cloud center. Future work should focus on better elucidating this relatively weak impact of below-cloud N_{CCN} compared to above-cloud N_{CCN} .~~

Beyond this corroboration of in situ findings, Θ nea major focus of this study was the dependence of aerosol – cloud relationships on environmental stability. Based on a k-means clustering analysis using LTS as the sole clustering variable, we stratified observations of the cloud deck with collocated above-cloud N_{CCN} retrievals into four clusters which turn out to be geographically distinct, with LTS increasing from the northwestern part of the SEA toward the southeastern part closest to the African coast. This increase in LTS aligns well with observed decreases in SST and CTH. ~~By constraining the meteorology~~ **Using this method**, we find that environmental stability is an important governing factor in determining the sensitivity of cloud properties to increases in above-cloud N_{CCN} . As the ~~atmosphere~~ **lower-tropospheric layer** becomes more stable, cloud sensitivity to increasing above-cloud N_{CCN} decreases until there is almost no response (cluster 4; Fig. 5d, h). ~~This suggests that~~ **Less stable environments promote greater vertical growth of the cloud layer and mixing led by cloud top entrainment instability (e.g., Mellado, 2017; Gupta et al., 2021). These is environments** thereby supports the modulation of cloud top properties by aerosols from the overlying smoke plume that are entrained into the cloud layer. The percent differences in ACI metrics between cluster 4 and cluster 1 are -73.9 % for ACI_{REF} and -74.3 % for ACI_{CDNC} , again indicating that ACIs depend strongly on environmental conditions. While we see from Fig. 4 that above-cloud ACIs are evident across the full data set, stratifying the data by LTS demonstrates the significant role that meteorology plays in determining how clouds respond to increases in above-cloud N_{CCN} . For example, comparing the full data set (Fig. 4a,b) to the cluster of data with the lowest mean LTS (Fig. 5a,e) ACI_{REF} increases from 0.093 to 0.161 (73.1 %) and ACI_{CDNC} increases from 0.275 to 0.452 (64.4 %). Therefore, stratifying data by environmental stability has a large impact on the magnitude, and arguably the accuracy, of the ACI metrics.

Further, we find that constraining the below-cloud N_{CCN} – cloud property relationship using LTS elucidates ACI relationships that are not evident when considering the CE data set as a whole. Observations shown in Fig. 7 suggest that at and within 5 km of cloud edges, below-cloud N_{CCN} have a nearly negligible impact on cloud top microphysical properties, which by itself is a physically implausible result. However, upon assigning CE observations to the clusters determined in Fig. 5, we find that cloud

sensitivity to increasing below-cloud N_{CCN} has the opposite dependence on LTS as for above-cloud N_{CCN} . That is, in more stable environments (cluster 4), decreased entrainment of above-cloud smoke aerosols into the cloud layer results in higher ACI metrics for below-cloud N_{CCN} than above-cloud N_{CCN} . Since high LTS promotes increased cloud fraction, selecting profiles at cloud edges with which to assess the simultaneous impact of above- and below-cloud N_{CCN} preferentially results in a subset of data with lower average LTS. Therefore, when considering all CE cases together, the stronger impact of below-cloud N_{CCN} for high LTS cases is masked. This finding speaks again to the importance of constraining environmental stability when assessing ACI and identifies a limitation of our methodology. Additionally, these stability-related findings corroborate those from ~~additional~~ other ORACLES ACI-focused studies. Using ORACLES 2016 in situ observations, Diamond et al. (2018) found a weaker relationship between cloud properties and above-cloud BBA compared to the below-cloud effect. Since cloud-focused in situ flight legs often target optically thick and continuous cloud segments, it is likely that these observations are characterized by a higher LTS than most of our CE cases.,—and similarly Moreover, a majority of the 2016 observations in this study are categorized by a high average LTS (Fig. 6), where we, like Diamond et al. (2018) also find stronger below-cloud ACI relationships than those observed above-cloud see above-cloud ACI relationships begin to weaken. Kacarab et al. (2020) discussed the sensitivity of ACI to velocity-limited and aerosol-limited regimes in the ORACLES 2017 observations, and this analysis indirectly suggests a dependence on updraft velocity via environmental stability. Future work exploring differences in aerosol properties, cloud properties, and other meteorological variables within each of these clusters could further assess and constrain ACI in this region.”

Section 4.2 was created to separate the original Section 4.1 into two separate sections. This section is titled “Reversals in expected patterns.” The following paragraph was added (Lines 601-611) to discuss patterns in cluster 4 of the new Fig. 9, showing how R_{eff} and N_d change with increasing below-cloud N_{CCN} in the highest LTS cluster. Additionally, the three new references in this paragraph were added to the reference list.

“A similar reversal in the expected response to increasing N_{CCN} is visible in cluster 4 of Fig. 9, though in this case it occurs at low N_{CCN} , and not within the highest concentration N_{CCN} bin. This increase in R_{eff} and decrease in N_d occurs for N_{CCN} bins between approximately $170\text{-}360\text{ cm}^{-3}$, representing relatively clean BL conditions. Therefore, it is unlikely that these patterns are attributable to the semi-direct effect of above-cloud BBA. Rather, this may be a case in which low N_{CCN} near cloud base

creates a low concentration of larger droplets that is maintained by the collision-coalescence process (Saleeby and Cotton, 2005) before N_{CCN} increases above 400 cm^{-3} . Populations of large droplets at cloud base have been observed in clean aerosol regions for convective clouds over the Amazon by Braga et al. (2017), and this effect has been hypothesized to be attributable to the presence of giant CCN (GCCN) by this and other studies (Yin et al., 2000; Saleeby and Cotton, 2005). It is likely that the below-cloud N_{CCN} population in this region includes sea salt particles, which are an aerosol type more likely to reach such sizes to be classified as GCCN. However, this remains a hypothesis to explain the increase in R_{eff} and decrease in N_d at low below-cloud N_{CCN} as the exact composition and size of below-cloud N_{CCN} is outside the scope of this analysis.”

The following edits were made in Section 4.3 in relation to the below-cloud N_{CCN} findings:

- Line 613-614: “The major implication of these results confirming those of an in situ-based study (Gupta et al., 2021) is that, **with the right considerations regarding environmental stability**, ACI can reliably be estimated using only these remote sensing-based observations.”
- Line 621-624: “...we found that changes in above-cloud N_{CCN} are more strongly related to changes in cloud top microphysical properties **under unstable conditions**, while ~~than~~ **changes in the below-cloud N_{CCN} have a more significant impact on cloud properties under stable conditions**. However, without vertically resolved N_{CCN} from the ML-CCN method, this **above- and below-cloud N_{CCN} distinction would not have been possible.**”
- Line 632-638: “**However, one important limitation inherent to this method is that the selection of cloud edge cases for assessing the simultaneous impact of above- and below-cloud N_{CCN} may preferentially create a subset of primarily low LTS observations which needs to be considered when interpreting results. Consequently,** ~~Lastly, the dependence of cloud sensitivity to increasing above-cloud N_{CCN} ACI on LTS speaks to the need to constrain future satellite observations by a **stability-related** parameter such as LTS to accurately represent meteorological impacts on ACI metrics, which may also impact their parameterization in models.~~”

The following edits were made in Section 5 in relation to the below-cloud N_{CCN} findings:

- Lines 648-663: “We found that our results align well with those of the in situ-based study (Gupta et al., 2021). That is, we see a decrease in R_{eff} and increase in N_d when

the BBA concentrations are significant within 100 m of the cloud top, and this finding is independent of horizontal proximity to cloud edge **and the magnitude of BL aerosol loading**. Using clear-sky, cloud-adjacent ML-GCN profiles, we examine the simultaneous impact of above- and below-cloud N_{CCN} and find that the relationship between cloud top microphysical properties and above-cloud N_{CCN} is stronger than their relationship with below-cloud N_{CCN} . This finding is independent of the magnitude of BL aerosol loading. Therefore, it appears that entrainment of BBA at cloud top in the SEA is a major control of cloud top microphysical properties. However, the dominance of this effect in comparison to that of below-cloud N_{CCN} remains an open question that would likely require modelling studies to further assess. Additionally, to constrain the impact of meteorology **environmental stability** we cluster the above-cloud **and cloud edge** data sets by LTS, finding that cloud sensitivity to increasing above- (**below-**)cloud N_{CCN} decreases (**increases**) as LTS increases. **Therefore, it appears that entrainment of above-cloud BBA into the stratocumulus cloud layer is a major control of cloud top microphysical properties under relatively unstable conditions, while the below-cloud N_{CCN} effect on cloud properties is stronger under more stable conditions.** The strongest $R_{eff} = N_{CCN}$ and $N_d = N_{CCN}$ relationships are found in the northwestern part of the ORAGLES region where average LTS is around 10 K, and the relationships weaken moving southeast towards the African coast. Therefore, while we do see evidence of an aerosol effect on cloud properties, this **both above- and below-cloud N_{CCN} effects are** is highly dependent on environmental stability.”

The following edits were made in the Abstract in relation to the below-cloud N_{CCN} findings:

- Lines 22-27: “Additionally, we find that **above-cloud N_{CCN} – cloud property relationships are similar for cloud edge and cloud center observations.** †The relationship between below-cloud N_{CCN} and cloud top properties is **strongly dependent on LTS, with ACI metrics increasing as LTS increases. This speaks to the dominance of above-cloud smoke entrainment as a modulator of stratocumulus cloud properties under unstable conditions, while below-cloud N_{CCN} nucleation dominates in stable environments.** weak and that above-cloud N_{CCN} – cloud property relationships are similar for cloud edge and cloud center observations.”